

# Investigation of biodegradable and biocompatible castor oil poly(mannitol-citric-sebacate) polyester as a drug carrier

P. S. Sathiskumar<sup>1</sup>, Sunita Chopra<sup>2</sup> and Giridhar Madras<sup>1,\*</sup>

<sup>1</sup>Department of Chemical Engineering, and

<sup>2</sup>Molecular Reproduction and Developmental Genetics, Indian Institute of Science, Bangalore 560 012, India

Castor oil-based poly(mannitol-citric sebacate) was synthesized by simple, catalyst-free melt condensation process using monomers having potential to be metabolized *in vivo*. The polymer was characterized using various techniques and the tensile and hydration properties of the polymers were also determined. The biocompatibility of the polymer was tested using human foreskin fibroblasts cells. The *in vitro* degradation studies show that the time for complete degradation of the polymer was more than 21 days. The usage of castor oil polyester as a drug carrier was analysed by doping the polymer with 5-fluorouracil model drug and the release rate was studied by varying the percentage loading of drugs and the pH of the PBS solution medium. The cumulative drug-release profiles exhibited a biphasic release with an initial burst release and cumulative 100% release within 42 h. To understand the role of the polymer as a drug carrier in the release behaviour, drug-release studies were conducted with another drug, isoniazid. The release behaviour of isoniazid drug from the same polymer matrix followed an *n*th order kinetic model and 100% cumulative release was achieved after 12 days. The variation in the release behaviour for two model drugs from the same polymer matrix suggests a strong interaction between the polymer and the drug molecule.

**Keywords:** Biodegradable, biocompatibility, castor oil polyesters, drug-delivery.

## Introduction

BIODEGRADABLE polymers have proven to be a versatile class of biomaterials in the field of temporary implants, tissue engineering and drug-delivery systems with different routes of administration. Conventional oral drug administration does not usually provide rate-controlled release as well as target specificity<sup>1</sup>. Oral and intravenous drug administration initially increases the drug concentration sharply at potentially toxic levels followed by main-

taining it at therapeutic level for a short period, which drops down to low levels until readministration. This problem can be overcome by shifting to local drug-delivery by controlled release systems using polymer-drug implants. These drug-delivery devices aid in the controlled release by providing therapeutic drug levels, restricting the drug-delivery to a specific site within the body and reducing the number of readministrations during treatment<sup>2,3</sup>. The use of biodegradable polymers in the drug-delivery implants has gained importance in recent years. The use of biodegradable polymer-drug implant systems for controlled release and target specificity in treating cancers and tumours has been studied and has shown promising results<sup>4-9</sup>.

Among the biodegradable polymers, aliphatic polyesters find potential applications as drug-delivery carriers in local drug-delivery systems for *in vivo* applications due to their degradability and biocompatibility<sup>8-10</sup>. Drug delivery from polymeric implants depends on the leaching ability of the drug, degradation of the polymer, and the crosslinks and swelling of the polymer. Aliphatic polyesters such as poly lactic acid (PLA), polyglycolic acid (PGA) and their copolymer poly(lactic-co-glycolic acid) (PLGA), though considered degradable hydrolytically, have biodegradation times varying in weeks to years, depending on the synthetic procedures<sup>11</sup>. These polymers on usage as drug carriers can complete their function for drug-delivery, but take a long time to degrade. 5-Fluorouracil (5-FU) is one of the most commonly used anticancer agents, but it is poorly absorbed after oral administration and thus local drug-delivery is the ideal way to overcome these disadvantages<sup>12,13</sup>.

In this present study, a soft and flexible thermoset castor oil-based poly(mannitol-citric-sebacate) (CO-p(MCS)) with rapid degradation property was synthesized by a simple, catalyst-free, inexpensive melt condensation polymerization process using sebacic acid (SA), citric acid (CA), mannitol and castor oil (CO) as monomers. The selection criteria chosen for the monomers were such that they should be: (i) nontoxic, inexpensive, readily available from renewable resources, (ii) multifunctional to form randomly crosslinked networks, (iii) allow forming easily hydrolysable ester linkages through polycondensation

\*For correspondence. (e-mail: giridhar@chemeng.iisc.ernet.in)

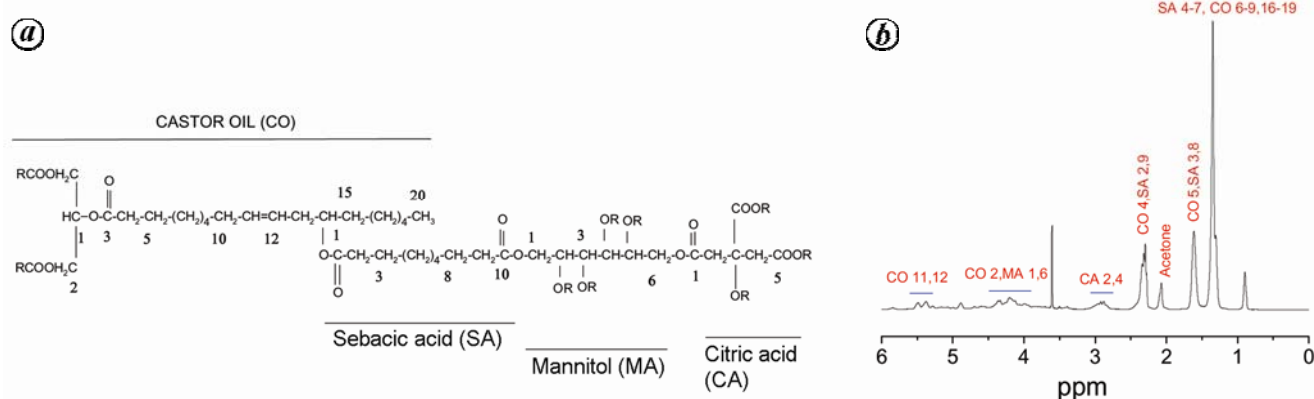


**Figure 1.** *a*, Castor oil based polyester (CO-p(MCS)) structure; *b*, <sup>1</sup>H NMR spectra of CO-p(MCS) in acetone.

reactions and (iv) biocompatible. The reason behind the selection of these monomers and the various types of polymers obtained along with their different physical and degradation properties is mentioned in our previous work<sup>14</sup>. The molecular structure of the synthesized polyester is shown in Figure 1a. The polymer synthesized was characterized by various techniques, including *in vitro* degradation behaviour in physiological conditions. The cytotoxicity of the polymer was studied using human foreskin fibroblast (HFF) cells. The usage of these polymers as drug carriers was studied by drug-delivery studies in physiological conditions using 5-FU and isoniazid (an anti-tuberculosis medication) as model drugs in PBS medium.

## Materials and methods

### Synthesis of castor oil-based poly(mannitol-citric-sebacate)

SA, CA, *d*-mannitol (MA) and CO were purchased from S.D. Fine Chemicals Ltd (India). Castor-oil-based polyester (CO-p(MCS)) was synthesized by the melt condensation polymerization technique using the above monomers. Initially, molar quantities of SA and CA (1.0 : 0.75 : 0.6 : 0.15/SA : CA : MA : CO) were taken in a three-necked round-bottom flask and the required quantity of CO was added. The mixture was allowed to react for 1 h at  $170 \pm 5^\circ\text{C}$  with continuous stirring and nitrogen gas purging to provide an inert atmosphere and to aid the removal of water formed during the reaction. After 1 h, mannitol was added to the reaction flask and the reaction was continued for 1 h at  $160 \pm 5^\circ\text{C}$ . The prepolymer formed was post-polymerized in a vacuum oven for 2 days at  $100^\circ\text{C}$  and 560 mmHg to form crosslinked polyester for polymer characterization and the prepolymer was taken directly for polymer–drug implants.

The polymer formed after the melt polymerization reaction will have unreacted functional groups in the

product and this is termed as a prepolymer. These prepolymers are not crosslinked and, therefore, soluble in solvents. This property of prepolymer solubility in solvents was utilized for NMR characterization. On subsequent curing under controlled conditions, the reaction attains completion and forms a solid mass, which is highly crosslinked and will not dissolve in any solvents. The cured polymers were used for drug-delivery, degradation and biocompatibility studies. For preparing the drug-loaded polymers, the prepolymer and drug were dissolved in ethanol and subsequently, ethanol was evaporated.

### Polymer characterization

<sup>1</sup>H-NMR spectra for the polymer were recorded on a Bruker NMR spectrometer at 400 MHz using acetone as solvent and tetramethylsilane (TMS) as the internal reference. Initially, the prepolymer was purified by dissolving the polymers in 1,4-dioxane (20 wt%) and precipitated in water–propanol (3 vol%) non-solvent mixture with continuous agitation, followed by filtration and freeze-drying at  $-90^\circ\text{C}$ . The cured polymer was subjected to Fourier transform infrared (FTIR) analysis by scanning thin films made out of cured polymer and KBr crystals using FTIR (Perkin Elmer) spectrometer over the  $4000\text{--}500\text{ cm}^{-1}$  range, at room temperature. To understand the thermal properties, the polymer sample was heated from  $-80^\circ\text{C}$  to  $150^\circ\text{C}$  at  $5^\circ\text{C}/\text{min}$  heating rate, cooled from  $150^\circ\text{C}$  to  $-80^\circ\text{C}$  at  $20^\circ\text{C}/\text{min}$  cooling rate and subsequently heated for a second cycle up to  $150^\circ\text{C}$  at  $5^\circ\text{C}/\text{min}$  heating rate in a Differential Scanning Calorimeter (Mettler Toledo DSC822<sup>o</sup>, USA) operating in a nitrogen atmosphere. The surface property of the polymer was analysed by contact-angle measurement using sessile drop method. Water droplets were carefully placed over the polymer surface and the images of the water–air–polymer interface were captured. These images were analysed using image analysis software to evaluate the initial water-in-air contact

angle. The hydration property was evaluated by incubating the polymer discs ( $\Phi$  10 mm  $\times$  2 mm) in Milli-Q water at 37°C. The increase in weight at specified intervals was measured by weighing the samples after wiping the surface moisture. After reaching the equilibrium percentage hydration, the polymer discs were dried to constant weight and the sol content of the polymer was calculated. Mechanical properties of the polyester were measured in tensile mode at room temperature using Universal Testing Machine (Zwick/Roell Z005, Germany) equipped with data-acquisition software. Dog-bone-shaped specimens ASTM standard D638 were prepared and tested at a strain rate of 10 mm/min to evaluate the elongation, tensile strength and Young's modulus of the polymer. The density of the polymer was measured using Archimedes' principle with water as the auxiliary liquid.

### *In vitro degradation*

The polymer specimens ( $\Phi$  10 mm  $\times$  2 mm) were immersed in 10 ml of phosphate buffer saline solution ( $n = 4$ ) and maintained at 37°C with continuous agitation. At specified intervals of time, the polymer discs were removed, washed with Milli-Q water and dried to constant weight under vacuum. The percentage degradation of the polymers in buffer saline solution was calculated by comparing the initial weight and the degraded weight measured at specified times.

### *Cell culture*

The cytotoxicity test is the first in a series of tests for evaluating the biocompatibility of a polymer in which the toxicity effect on the mammalian cells due to the presence of the polymer or its degradation products is studied<sup>15</sup>. Initially, the polymer specimen ( $\Phi$  10 mm  $\times$  2 mm) was sterilized by rinsing with absolute ethanol and UV radiation for 30 min. Primary HFF cells were used in this study for evaluating the biocompatibility. These cells were grown in high-glucose Dulbecco's minimal essential medium (DMEM; Sigma) supplemented with 10% (v/v) foetal bovine serum (Invitrogen), 100  $\mu$ g/ml streptomycin (Invitrogen) and 100 U/ml penicillin (Invitrogen)<sup>16</sup>. After growth, these cells were harvested using trypsin (0.025%)/EDTA (0.01%), and these cells were resuspended by adding an equal volume of the medium. The suspended fibroblast cells in the medium were seeded in two polystyrene sterile tissue-culture dishes (Nunc) at very low density (15–20% confluence), and 15 ml of DMEM medium (supplemented with FBS, streptomycin, penicillin) was added. One petri dish served as the negative control and the other dish was loaded with sterilized polymer sample to study the cytotoxicity effect of the polymer. Both the disks were incubated at 37°C and 5% CO<sub>2</sub>, and the cells were allowed to grow to form a con-

fluent monolayer. The cells were observed for growth in the dish through an inverted microscope every two days and the medium was replaced with a fresh medium on alternate days. At the end of 7 days, the cells were imaged for accessing the morphology and confluence at 10 $\times$  magnification using a Leica DMIRM inverted microscope and Leica Quis Software.

### *Scaffold fabrication*

Porous scaffold from the polyester was fabricated using the salt-leaching technique utilizing the solubility of prepolymer in different solvents<sup>17</sup>. The prepolymer was dissolved in 1,4-dioxane separately to form 25 wt% solution. Sieved salt was added to this solution to form a slurry (25% w/v). The slurry was transferred to Teflon moulds and the solvent was allowed to evaporate slowly at 90°C. After solvent evaporation for 24 h, the moulds were transferred to a vacuum oven and the polymers were cured at 560 mmHg vacuum and 100°C for 3 days. The cured salt-filled polymers were demoulded and cut into square pieces of 2 cm  $\times$  2 cm. These samples were leached out of salt by incubating the polymer in Milli-Q water and replacing the water medium every 12 h for 4 days. The resulting porous polymer was freeze-dried at -90°C and stored in desiccators. These porous scaffolds were sputter-coated with gold and examined under a scanning electron microscope (FEI, QUANTA, USA) at 5 kV. The images were analysed for small-sized pores using image analysis software.

### *Drug release studies*

*Preparation of drug-polymer matrix:* The prepolymer was dissolved in absolute ethanol to form a solution (20 %wt/vol). 5-FU and isoniazid were taken for the analysis. The required quantity of drug was added to the polymer solution and stirred. The polymer-drug solution was transferred to Teflon moulds and the solvent was allowed to evaporate slowly for 24 h. After the solution became viscous, the moulds were transferred to an oven for vacuum curing at 660 mmHg vacuum and 100°C for 4 days. The cured drug-polymer matrix samples were analysed for drug-loading efficiency. Small polymer-drug matrix discs were weighed and placed in 100 ml of basic solution (NaOH solution) and allowed for complete dissolution of the polymer and the drug<sup>18</sup>. The supernatant liquid was analysed for the drug quantity using the absorbance level at the respective  $\lambda_{\text{max}}$  for different drugs measured with a UV-Vis spectrophotometer.

*Drug delivery from drug-polymer matrix:* Phosphate buffer solutions with different pH values (7.4, 6.8 and 5.5) were prepared using monosodium diphosphate and disodium phosphate. Samples ( $\Phi$  10 mm  $\times$  2 mm) were

punched out from polymer–drug composites and dipped in 100 ml of 0.1 M PBS solution maintained at 37°C with continuous agitation. At specified time intervals, 1 ml of release medium was taken out and analysed for the drug level in the medium using UV-Vis spectrophotometer (UV1700 Pharmaspec, Shimadzu). The absorbance at 268 nm for 5-FU and 263 nm for isoniazid was measured, and the amount of drug released in the media was evaluated from the predetermined calibration curve. The cumulative drug-release percentage was calculated to establish the drug-release profile of the prepared drug–polymer matrix.

## Results and discussion

### Polymer synthesis and characterization

CO-p(MCS) was synthesized by catalyst-free melt polycondensation reaction without extreme synthesis conditions in a single-step process, which avoids toxicity being induced by most of the catalyst/initiators. CO alone was allowed to react with diacids for 1 h due to the lower reactivity of CO than *d*-mannitol. The schematic representation of the reaction between all the monomers is explained in our previous work<sup>14</sup>. The prepolymer synthesized was found to be soluble in methanol, ethanol, acetone, 1,4 dioxane. Figure 1 *a* shows the structure of the synthesized polymer and Figure 1 *b* shows the spectrum of <sup>1</sup>H-NMR of CO-p(MCS) in acetone, which is in accordance with the structure. The presence of CO in the compound was confirmed by the peaks of the protons of the unsaturated alkene group (CO 11, 12) and the terminal methyl group of ricinoleate (CO 20) at 5.35–5.55 and 0.9 ppm respectively<sup>19</sup>. Methylene (MA 1,6) and methine (MA 2–5) groups of mannitol were observed at 3.75–4.5 ppm and 4.7–5.0 ppm respectively<sup>16</sup>. The multiple peaks between 2.8 and 2.95 ppm were due to the methylene protons (CA 2,4) in CA<sup>17</sup>.

The synthesis and characterization of the polymers have been discussed extensively in our previous work<sup>14</sup>. Despite the small quantity of CO, crosslinked structures are formed due to the trifunctionality of CO. The NMR spectrum for this prepolymer has peaks common for many of its monomers. CO can be easily identified in the <sup>1</sup>H-NMR spectrum by the double-bond peaks specific to it. However, the peaks of SA CH<sub>2</sub> group and *d*-mannitol CH and CH<sub>2</sub> groups are merged with similar groups available in CO, and hence qualitative analysis could not be used for determining the monomer ratios in the prepolymer. However, it may be presumed that all the monomers are incorporated in the polymer because the mass loss during curing is less than 2%. The NMR spectra are given for the prepolymer and the polymer becomes crosslinked after curing. The crosslink density (*n*) and molecular weight between crosslinks of the polymer after

curing were calculated to be  $130.5 \pm 16.1$  and  $8223.5 \pm 117.7$ , respectively<sup>14</sup>.

The cured polymer was characterized by FTIR analysis by identifying the peaks for the specific functional groups in the IR spectrum over the 4000–500 cm<sup>-1</sup> range. Figure 2 *a* shows the FTIR spectrum for the synthesized CO-p(MCS) polymer. The peak at 1740 cm<sup>-1</sup> corresponds to ester C=O group stretching, and the peaks at 1635 cm<sup>-1</sup> and 1380 cm<sup>-1</sup> correspond to the double bond (C=C) and the C–H bending of end methyl group in CO respectively. Figure 2 *b* shows the DSC thermogram and the glass transition temperature (*T*<sub>g</sub>) of the polymers was derived from the derivative of the thermogram. Glass transition temperature for this polymer is –19.5°C, which indicates that the polymer is rubbery at physiological temperatures. Surface property measurement done on the flat polymer (CO-p(MCS)) surface provides a contact angle of 57°, which indicates that the surface is sufficiently hydrophilic and is advantageous for the interaction with biological molecules. Figure 2 *c* shows the rate of change of hydration level for the polymer synthesized. The equilibrium hydration level of the polymer in Milli-Q water is 3.09%, which indicates that the polymer does not easily hydrolyse in the presence of Milli-Q water. Figure 2 *d* shows the representative tensile mode stress versus strain plots for the synthesized CO-p(MCS) polymer. The average Young's modulus, ultimate tensile strength (UTS), elongation at break and other properties of the polymer are mentioned in Table 1 (ref. 14).

### In vitro degradation

Aliphatic, biodegradable polyesters when placed in an aqueous medium start degrading due to hydrolysis. CO-p(MCS) was tested for its degradation behaviour under physiological conditions using PBS solution (pH 7.4) at 37°C. The degradation behaviour of the polyester can be analysed by the change in molecular weight, solution viscosity as well as mass-loss measurements<sup>20</sup>. As the synthesized cured polymer is crosslinked, the first two methods cannot be used and hence mass-loss measurements were carried out to determine the degradation

**Table 1.** Physical, mechanical and thermal properties of CO-p(MCS) polyester

Property	Value
Young's modulus (MPa)	0.97 ± 0.12
Ultimate tensile strength (MPa)	0.34 ± 0.02
Elongation at break (%)	52 ± 3
Density (g/cc)	1.073 ± 0.002
Contact angle (°)	57.1 ± 5.3
<i>T</i> <sub>g</sub> (°C)	–19.5
Equilibrium hydration by mass (%)	3.09 ± 0.23
Sol content by mass (%)	5.19 ± 0.12

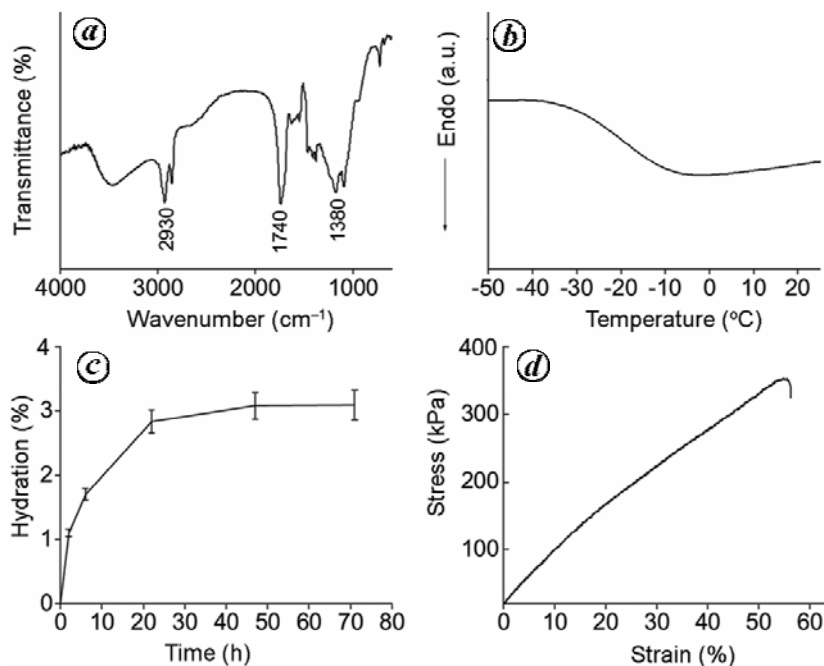


**Figure 2.** Cured CO-p(MCS) polymer characterization. *a*, FTIR spectrum; *b*, DSC thermogram; *c*, Hydration profile; *d*, Stress–strain curve.

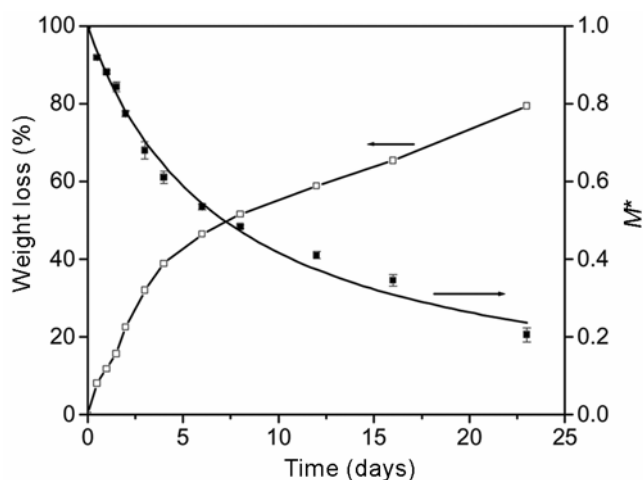


**Figure 3.** CO-p(MCS) degradation profile in PBS solution at pH 7.4 and the best fit for degradation using normalized weight ( $M^*$ ).

behaviour. The results of the degradation are shown in Figure 3 as the variation of the weight loss of the polymer with incubation time. The degradation mechanism of the polymer in aqueous medium involves a combination of diffusion, chemical reaction and dissolution process. Assuming that the diffusion and dissolution parameters combine with the reaction rate constant, the degradation mechanism can be represented by a rate equation

$$-\frac{dM}{dt} = kM^n, \quad (1)$$

where  $M$  is the weight of the sample,  $n$  the order of the degradation process and  $k$  the degradation rate constant.

Figure 3 shows the best fit degradation profile also for CO-p(MCS) polymer by solving eq. (1) using normalized weight  $M^*$  ( $M^* = M/M_0$ ), and  $M^* = 1$  at  $t = 0$ , where  $M_0$  is the initial weight of the sample. The best fit of the profile gives an apparent degradation constant ( $k$ ) value of  $1.30 \pm 0.07 \text{ (g}^{(n-1)} \cdot \text{day)}^{-1}$  and order of the degradation process as 2.0.

### Cell culture

Cell-culture test was used to evaluate the cytotoxicity of the CO-p(MCS) polymer using HFF cells. In the cell-culture method, the performance of cells such as growth pattern and morphology in the presence of any external material (polymer) was compared with a negative control. The negative control in this experiment was a cell culture in polystyrene dish which is compatible with cells. It was noticed on the second day of observation that the cells were attached at the bottom of both the dishes. Figure 4 shows the optical photomicrographs of HFF cell growth after 7 days of incubation in the presence of polymer and in the negative control. The images show that the cell morphology was similar in both the dishes and had a complete confluence in the dish. The morphology of the cells proves that they had survived in the presence of the polymer, were attached to the bottom of the dish and finally grew to occupy the whole area (full confluence) with spindle-shaped morphology. The results indicate that the polymer does not release any inhibitory leachate to the medium that is toxic and thus the polymer was found to be non-cytotoxic.

*Scaffold fabrication*

CO-p(MCS) polymer was fabricated as a porous sponge-like scaffold by the salt leaching technique. The SEM image of the scaffold (Figure 5) shows interconnected pores between the polymer networks. The SEM image reveals that many micropores were seen along with macropores in the scaffold and the size of the micropores was found to be  $20 \pm 10 \mu\text{m}$ . These micropores will serve as a passage route for the nutrients, deep inside the polymer scaffold, which are required for cell growth in tissue engineering<sup>17</sup>. The scaffold type of polymer network can be used for various vascular graft/tissue-engineering applications. For tissue-engineering applications, the excess hydroxyl/carboxyl groups available in the polymer backbone chain can be utilized as moieties for potential modification. Peptides or proteins can be incorporated into the polyester network using these functionalities to derive a particular cell response.

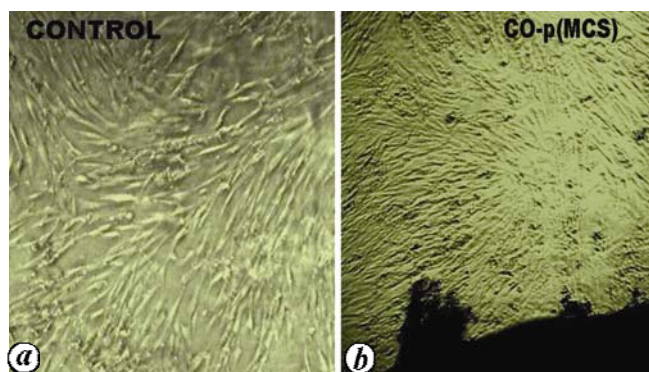


**Figure 4.** Photomicrographs of human foreskin fibroblast cells culture: *a*, Negative control; *b*, In the presence of CO-p(MCS) polymer.

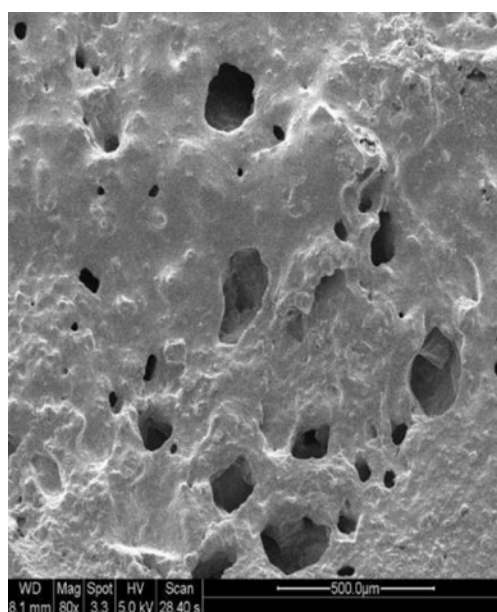


**Figure 5.** SEM image of porous CO-p(MCS) polymer scaffold.

*Drug-delivery studies*

Controlled release is desirable in any drug release application. The drug encapsulated in the degradable polymer implants allows for its controlled release, but the degradation of the polymer alone is not responsible for controlled release. The dissolution of the drug in the medium and the diffusion of the medium through the matrix, swelling of the polymer and crosslink density also play a role in manipulating the drug-release profiles<sup>20,21</sup>. The most desirable release profile from a polymer–drug implant is a constant release rate, but most of the drug implants have varying release rates. In many cases, the release profile shows biphasic expulsions, the first being a burst release of drug and the second is a usually constant release profile controlled by degradation and diffusion mechanism. The initial burst release of the drug is mostly due to the fast dissolution of the drug from the implant surface, as there is no requirement of diffusion of medium inside the implant. This behaviour indicates the dispersion of the drug molecules in the polymer matrix.

The initial burst will be higher if it fills the surface more, whereas the burst release will be lower if there is an even distribution of the drug inside the matrix also. Thus the interaction of the polymer with the drug molecule plays a role in evenly distributing the drug molecule throughout the matrix. For crosslinked polymers, the initial hydrolysis changes the crosslink density of the polymer matrix, which does not necessarily involve weight loss. This results in an increasing diffusion of the medium inside the matrix and increased permeation rate of the drug caused by the gradually decreasing crosslink density<sup>13</sup>. Incorporation of the drug molecules in the polymer matrix increases the degradation of the polymer after the initial expulsion of the drug molecules from the matrix<sup>20</sup>. The expulsion of the drug relaxes the polymer network due to the increased free space, which allows for easy diffusion of the medium into the matrix. The availability of the medium inside the matrix increases the hydrolysis reaction, which causes faster degradation.

In the present work, the synthesized CO-p(MCS) rapid degrading polyester was used as a drug carrier and the drug release behaviour from these polymers in PBS medium was studied using two model drugs, namely 5-FU and isoniazid. Loading efficiency of the drugs in the polymer was found to be between 87% and 92% for various loadings.

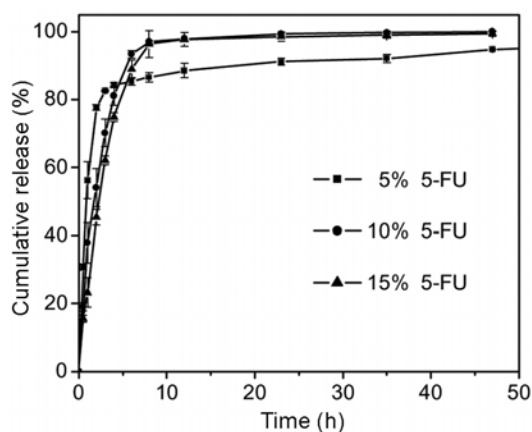
*Effect of drug loading*

Figure 6 shows the cumulative 5-FU drug release profile from CO-p(MCS)–5-FU implants for different drug loadings in the polymer. Drug release from the polymer implant shows that the release profile has burst release in the initial phase and thereafter a constant release for 5-FU drug. The 100% cumulative drug release of the drug from the implants happens within 48 h. As noted, the initial

burst release could be due to rapid dissolution of drug molecules from the exposed surface. Similar type of initial burst behaviour was observed with 5-FU drug from other polymer matrices and this characteristic of *in vitro* drug burst release is a common phenomenon in many drug-delivery systems<sup>10,22</sup>. The pCCP:SA matrix with BCNU drug is a commercially available drug-delivery system known as 'Gliadel' and its drug-release profile also shows a similar initial burst behaviour<sup>23</sup>. For higher drug loadings, the initial release rate of the drug is smaller, which eventually increases in due course of time and this has been also observed in other polymer systems with 5-FU drug<sup>10</sup>. This may be due to the comparatively higher distribution of the drug inside the matrix as the drug content increases and, therefore, the initial diffusion of water inside the matrix controls the initial rate for higher loading matrices. As the matrix releases the drug, more void pathways form inside the matrix, which increases the diffusion of medium inside and the drug solution outside resulting in increased release profile<sup>20</sup>.

#### Effect of different pH values

Similar drug-release studies were conducted using CO-p(MCS) polymer-drug implants (5% 5-FU loading) in PBS medium with three different pH values at 37°C. The reason for this is that though the pH of the body fluid (blood) is 7.4, the fluid around any inflammation due to ailments in the body will have a slightly acidic value, and these studies were conducted in release medium of pH 6.8 and 5.5 to understand the variation of release profiles for varying pH conditions. Figure 7 shows the variation of 5-FU release profile for different pH values of the medium. The release profiles indicate that as the pH of the medium decreases (being acidic), the initial drug-release rate also comparatively decreases. The reason for this behaviour is that in acidic medium the polymer is hydrolytically stable and the initial rate of hydrolytic



**Figure 6.** Drug-release profiles from CO-p(MCS)-5-FU drug implants in PBS medium at pH of 7.4 for different drug loadings.

chain cleavage will be smaller, which decreases drug release from the matrix. This type of behaviour having lesser drug-release rate from the polymer matrix in acidic medium was also observed in other polymer-drug matrices<sup>18</sup>.

#### Drug release with isoniazid

Drug-release studies in PBS medium of pH 7.4 were conducted with the second model drug, isoniazid, at 5 wt% loading to understand the role of the polymer in the release behaviour due to its interaction with the drug. Figure 8 shows the release profile of isoniazid from the same polymer compared with the 5-FU drug release pattern. The 100% cumulative release for this drug from the implant occurs at the 16th day. The drug-delivery from CO-p(MCS)-isoniazid matrix indicates a release profile without any burst release, which shows that the drug is evenly distributed deep inside the matrix. This may be possible due to the different kind of polymer-drug interaction during the preparation of implants. It was observed that swelling of the polymer during the analysis period was small and since the release profile does not show burst release, the profile was fitted by a kinetic model

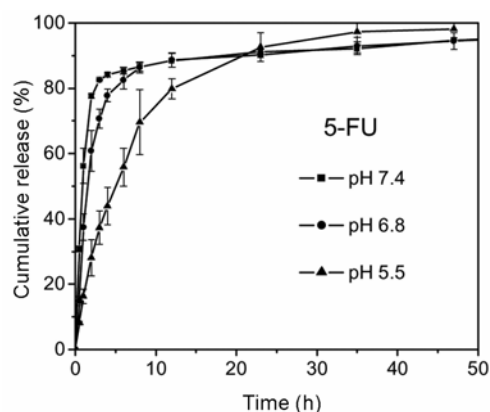


**Figure 7.** Drug-release profiles from CO-p(MCS)-5-FU drug implants (5% drug loading) in PBS medium with pH, 7.4, 6.8 and 5.5.

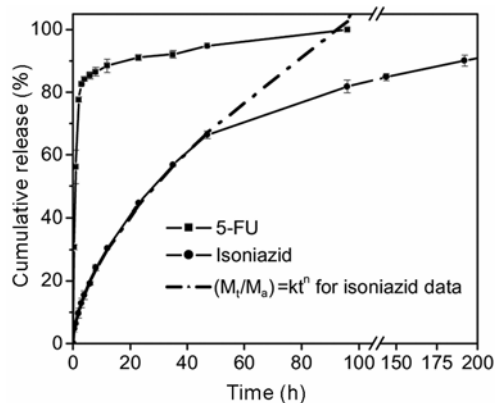


**Figure 8.** Comparison of drug-release profiles from CO-p(MCS)-5-FU drug implants for two different drugs (5-FU and isoniazid) in PBS medium of 7.4 and drug loading of 5%.

proposed for solute release from swellable devices<sup>24</sup>. This model, as given as eq. (2), provides information about the mechanism behind the release behaviour. The model explains that the prevailing mechanism for drug release is a coupling of diffusion and macromolecular relaxation.

The drug diffuses outward with a kinetic behaviour, which is dependent on the relative ratio of diffusion and relaxation.

$$\frac{M_t}{M_\infty} = kt^n \text{ valid for } \frac{M_t}{M_\infty} \leq 0.6. \quad (2)$$

A value of 0.5 for  $n$  denotes the Fickian diffusion as the drug-release mechanism, whereas a value of 1.0 for  $n$  denotes macromolecular relaxation mechanism. A value between 0.5 and 1.0 shows that the drug release is influenced by both the phenomena. It was shown that the drug-release profile for isoniazid follows eq. (2) with  $n$  value of 0.60 and  $k$  value of  $6.84 \pm 0.15 \text{ s}^{-n}$ , as seen from Figure 8, which indicates that both diffusion and relaxation mechanisms are responsible for the drug-release profile.

The distribution of 5-FU drug in the sample was not uniform throughout, with most of the drug available on the surface. On exposure to the PBS medium, the immediate dissolution of the drug in the medium also can be a reason for the rapid release. However, in the case of isoniazid, the drug penetrated deep inside the matrix and, therefore, rapid dissolution and release were not observed.

## Conclusion

We have synthesized CO-p(MCS) polymers that can be used as drug implants. A mass loss of 80% was observed in 25 days for this polymer. The study with polymer-5-FU implants shows that the drug release has a biphasic nature, whereas the implant with isoniazid shows a controlled release profile for a period of 16 days. The CO-p(MCS) polymer has good biocompatibility for HFF cells and can be used as drug implants for local delivery.

1. Edlund, U. and Albertsson, A. C., Degradable polymer microspheres for controlled drug delivery. In *Degradable Aliphatic Polyesters*, Springer, Berlin, 2002, vol. 157, pp. 67–112.
2. Uhrich, K. E., Cannizzaro, S. M., Langer, R. S. and Shakesheff, K. M., Polymeric systems for controlled drug release. *Chem. Rev.*, 1999, **99**, 3181–3198.
3. Brouwers, J. R. B. J., Advanced and controlled drug-delivery systems in clinical disease management. *Pharm. World Sci.*, 1996, **18**, 153–162.
4. Zhou, S., Deng, X., Yuan, M. and Li, X., Investigation on preparation and protein release of biodegradable polymer microspheres as drug-delivery system. *J. Appl. Polym. Sci.*, 2002, **84**, 778–784.
5. Bai, X.-L., Yang, Y.-Y., Chung, T.-S., Ng, S. and Heller, J., Effect of polymer compositions on the fabrication of poly(ortho-ester) microspheres for controlled release of protein. *J. Appl. Polym. Sci.*, 2001, **80**, 1630–1642.
6. Azab, A. K., Kleinstern, J., Doviner, V., Orkin, B., Srebnik, M., Nissan, A. and Rubinstein, A., Prevention of tumor recurrence and distant metastasis formation in a breast cancer mouse model by

- biodegradable implant of 131 Inorcholesterol. *J. Control. Release*, 2007, **123**, 116–122.
7. Cheung, R., Ying, Y., Rauth, A., Marcon, N. and Yuwu, X., Biodegradable dextran-based microspheres for delivery of anticancer drug mitomycin C. *Biomaterials*, 2005, **26**, 5375–5385.
8. Liu, J., Meisner, D., Kwong, E., Wu, X. Y. and Johnston, M. R., A novel translymphatic drug-delivery system: implantable gelatin sponge impregnated with PLGA–paclitaxel microspheres. *Biomaterials*, 2007, **28**, 3236–3244.
9. Brem, H., Polymers to treat brain tumours. *Biomaterials*, 1990, **11**, 699–701.
10. Sun, Z.-J. *et al.*, The application of poly(glycerol–sebacate) as biodegradable drug carrier. *Biomaterials*, 2009, **30**, 5209–5214.
11. Gunatillake, P. A., Adhikari, R. and Gadegaard, N., Biodegradable synthetic polymers for tissue engineering. *Eur. Cells Mater.*, 2003, **5**, 1–16.
12. Diasio, R. B. and Harris, B. E., Clinical pharmacology of 5-fluorouracil. *Clin. Pharmacokinet.*, 1989, **16**, 215–237.
13. Heller, J. *et al.*, Use of poly(ortho esters) for the controlled release of 5-fluorouracil and a LHRH analogue. *J. Control. Release*, 1987, **6**, 217–224.
14. Sathiskumar, P. S. and Madras, G., Synthesis, characterization, degradation of biodegradable castor oil based polyesters. *Polym. Degrad. Stabil.*, 2011, **96**, 1695–1704.
15. Katti, D. S., Lakshmi, S., Langer, R. and Laurencin, C. T., Toxicity, biodegradation and elimination of polyanhydrides. *Adv. Drug Deliv. Rev.*, 2002, **54**, 933–961.
16. Bruggeman, J. P., de Bruin, B.-J., Bettinger, C. J. and Langer, R., Biodegradable poly(polyol sebacate) polymers. *Biomaterials*, 2008, **29**, 4726–4735.
17. Yang, J., Webb, A. R., Pickerill, S. J., Hageman, G. and Ameer, G. A., Synthesis and evaluation of poly(diols citrate) biodegradable elastomers. *Biomaterials*, 2006, **27**, 1889–1898.
18. Kenawy, E.-R., Abdel-Hay, F., El-Newehy, M. and Ottenbrite, R. M., Effect of pH on the drug release rate from a new polymer–drug conjugate system. *Polym. Int.*, 2008, **57**, 85–91.
19. Yeganeh, H. and Hojati-Talemi, P., Preparation and properties of novel biodegradable polyurethane networks based on castor oil and poly(ethylene glycol). *Polym. Degrad. Stabil.*, 2007, **92**, 480–489.
20. Li, X., Deng, X., Yuan, M., Xiong, C., Huang, Z., Zhang, Y. and Jia, W., *In vitro* degradation and release profiles of poly-DL-lactide-poly(ethylene glycol) microspheres with entrapped proteins. *J. Appl. Polym. Sci.*, 2000, **78**, 140–148.
21. Freiberg, S. and Zhu, X. X., Polymer microspheres for controlled drug release. *Int. J. Pharma.*, 2004, **282**, 1–18.
22. Kim, G. Y., Tyler, B. M., Tupper, M. M., Karp, J. M., Langer, R. S., Brem, H. and Cima, M. J., Resorbable polymer microchips releasing BCNU inhibit tumor growth in the rat 9L flank model. *J. Control. Release*, 2007, **123**, 172–178.
23. Fung, L. K., Shin, M., Tyler, B., Brem, H. and Saltzman, W. M., Chemotherapeutic drugs released from polymers: distribution of 1,3-bis(2-chloroethyl)-1-nitrosourea in the rat brain. *Pharm. Res.*, 1996, **13**(5), 671–682.
24. Ritger, P. L. and Peppas, N. A., A simple equation for description of solute release II. Fickian and anomalous release from swellable devices. *J. Control. Rel.*, 1987, **5**, 37–42.

**ACKNOWLEDGEMENTS.** We thank the NMR Research Centre, Materials Engineering Department, Organic Chemistry Department, Material Research Centre and Centre for Nanoscience and Engineering, Indian Institute of Science (IISc), Bangalore for providing the necessary facilities. We also thank Prof. P. Kondaiah, MRDG, IISc for providing facilities and technical support for cell-culture tests, and the Department of Biotechnology, New Delhi for financial support.